

THE APPLICATION OF OTR-ODR INTERFEROMETRY TO THE MEASUREMENT OF THE DIVERGENCE OF LOW ENERGY ELECTRON BEAMS

A. Shkvarunets*, J. Harris, J. Neumann, D. Feldman, P. O'Shea, Institute for Plasma Research,
 University of Maryland, College Park, MD 20742,
 R. Fiorito, Department of Physics, Catholic University of America, Washington, DC 20064

Abstract

Optical Transition Radiation (OTR) interferometry has been shown to be a useful diagnostic to measure the divergence of electron beams with energies in the range of 15-100 MeV. A limitation of this method is due to beam scattering in the first foil of the interferometer. To mitigate this undesirable effect we propose to use a perforated first foil in the interferometer. In this case a substantial fraction of the unscattered beam electrons passing through the holes will produce Optical Diffraction Radiation (ODR). The total radiation produced from the first and second foils will be coherent ODR and OTR from unscattered electrons and incoherent ODR and OTR from heavily scattered electrons in the first foil. Such an ODR-OTR interferometer is being designed to measure the divergence at the University of Maryland's Infrared Free Electron Laser (MIRFEL) experiment. Calculations show that the method is capable of measuring beam divergences of the order of one milliradian for beam energies less than 10 MeV.

1 INTRODUCTION

OTR interferometry is a proven method for measuring the rms emittances of relativistic electron beams with energies ranging from 15-100 MeV [1]. In this technique two parallel thin foils, oriented at 45 degrees with respect to the electron beam, produce forward and backward directed OTR. When the distance between the foils is comparable to the vacuum coherence length $L \sim \gamma^2 \lambda$, interference fringes are observed whose visibility is a function of the rms beam divergence.

Scattering in the first foil of the interferometer limits this method to beam energies above about 10 MeV. When the energy of the electron beam falls below about 10 MeV and the rms divergence of the beam is smaller than about $0.05/\gamma$, it becomes very difficult to design a foil with less scattering than the divergence of the beam. To overcome this limitation, we plan to use a *perforated* first foil as shown in Figure 1. The total output light intensity distribution observed is the coherent sum of the intensities of ODR and OTR produced by the unscattered and scattered portions of the beam.

By proper choice of the first foil thickness, the inter-foil spacing, the size, number and spacing of the holes and the band pass of the imaging optics, interference fringes

from the unscattered electrons can be seen above the background light produced from the scattered portion of beam. The rms divergence of the unperturbed beam can be measured from the visibility of the interference fringes. In addition, the orthogonal (x, y) components of the divergence can be separately obtained by observing polarized interferences when the beam is focused to either an x or y waist condition [1].

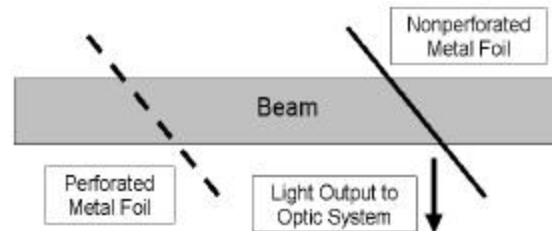


Figure 1: Schematic of ODR-OTR interferometer

2 APPROACH

In order to design the ODR-OTR interferometer to be sensitive to the expected 2 mrad beam divergence of the University of Maryland's 8 MeV electron beam accelerator, we have developed two computer codes.

Code (1) calculates the ODR and OTR intensity distributions produced by unscattered (U) and scattered (S) beams as shown in Figure 2.

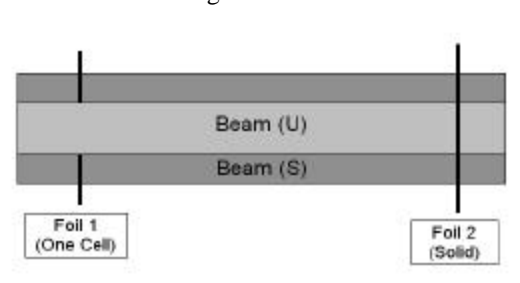


Figure 2: An expanded view of one of the foil cells

Code (2) calculates the coherent addition of ODR and OTR radiation fields produced at foils 1 and 2 by beams (U) and beam (S) which are assumed to have divergences σ_U and σ_S , respectively.

*shkvar@glue.umd.edu

2.1 Optical Diffraction Radiation - Code (1)

Following Ter-Mikelian [2] we assume that the optical diffraction radiation produced by electrons passing through the perforated foil can be calculated by applying Huygens Principle to the virtual photon field accompanying each electron (Weizsäcker-Williams method of virtual quanta). The virtual photons are scattered or diffracted by the circular hole and produce real photons at a screen downstream from the foil. The distribution of the field from the electrons at this screen is then given by the Huygens Fresnel Integral

$$U_{x,y} = \frac{k}{2\pi i} \int_{S_f} \frac{u_{x,y} e^{ikR} \cos \mathbf{q}}{R} dS_f,$$

where $U_{x,y}$ is any field component, $k=\omega/c$, R is the distance from S_f the differential element of area of the foil and $u_{x,y}$ is the Fourier component of the free space radial field of the electron given by:

$$u_{x,y} = \frac{x, y}{\sqrt{x^2 + y^2}} \frac{e\mathbf{a}}{p v} K_1(\alpha r)$$

where $\alpha = \omega/(\gamma v)$, v is the electron velocity and K_1 is the Hankel function with imaginary argument.

2.2 ODR - OTR Interferences - Code (2)

Code (2) calculates the total x or y component of the two foil light intensity distribution given by:

$$I_{Total} = \{I_{1U} + I_{2U} - \cos \Psi \sum_U E_{1e} \cdot E_{2e}\} \\ + \{I_{1S} + I_{2S} - \cos \Psi \sum_S E_{1e} \cdot E_{2e}\} \quad (1)$$

where $I_{n,B} = \Sigma (E_{ne,B})^2/2$ are the x or y intensity components from foils $n = 1,2$ for beams $B = U, S$; E_{ne} are the x or y components of the radiation field for a single electron produced by foils 1 and 2 calculated using Code (1); and the phase

$$\Psi = (\mathbf{w}d/c) (\mathbf{b}^{-1} \cos^{-1} \mathbf{q}_e - \cos(\mathbf{q} - \mathbf{q}_e) / \cos \mathbf{q}_e)$$

where d is the spacing between the foils, $\beta=v/c$, θ_e is the electron trajectory angle within the beam and θ is the observation angle.

The effect of beam divergence on the interference intensity pattern is taken into account by numerically convolving the intensity given above in Eq. (1) with a Gaussian distribution of electron angles:

$$P(\mathbf{s}_x, \mathbf{q}_x; \mathbf{s}_y, \mathbf{q}_y) = \exp(-\mathbf{q}_x^2 / 2\mathbf{s}_x^2) \cdot \exp(-\mathbf{q}_y^2 / 2\mathbf{s}_y^2),$$

where $\sigma_{x,y}$ are the x, y rms beam divergences and $\theta_{x,y}$ the angles of observation projected onto the plane of the detector.

If $\sigma_{x,y} \ll \gamma^{-1}$, the angle of peak emission for OTR and ODR, then the radiation fields at the observation plane $E_{1,2e}(\sigma_{x,y}, \theta_{x,y})$ are slowly varying functions of $\theta_{x,y}$ and hence are nearly independent of the beam divergences $\sigma_{x,y}$. Then only the phase term Ψ will be sensitive to beam divergence. The presence of beam divergence produces a reduction in the interference fringe visibility.

3 COMPUTATIONAL RESULTS

3.1 Code (1) Results

The Results of Code (1) are presented in Fig. 3 for a beam energy of 8 MeV. A perforation ratio (area of holes to foil area) of 0.45 was used. Code (1) was tested in cases for which theoretical formulas for ODR were available Refs. [2-4], and found to be in excellent agreement with the theoretical calculations in all cases.

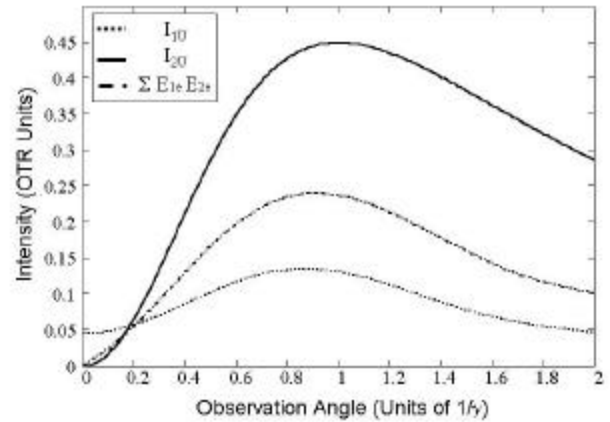


Figure 3: ODR and OTR intensities from the first and second foils for the unscattered portion of the beam passing through the holes (beam U), i.e. I_{1U} , I_{2U} and the first summation term $\sum S E_{1e} E_{2e}$ in Equation (1).

3.2. Code (2) Results

The results of Code 2 are given in Figs 4, 5 and 6. The observation wavelength $\lambda = 750$ nm, the bandpass $\Delta\lambda = 40$ nm and the beam divergence due to scattering in foil 1, $\sigma_s = 10$ mrad. Under these conditions the OTR produced by the scattered beam is essentially incoherent and forms a background above which the interference fringes from the unscattered beam are visible. The effects of unscattered beam divergences $\sigma_U = 0.5 - 8$ mrad are shown.

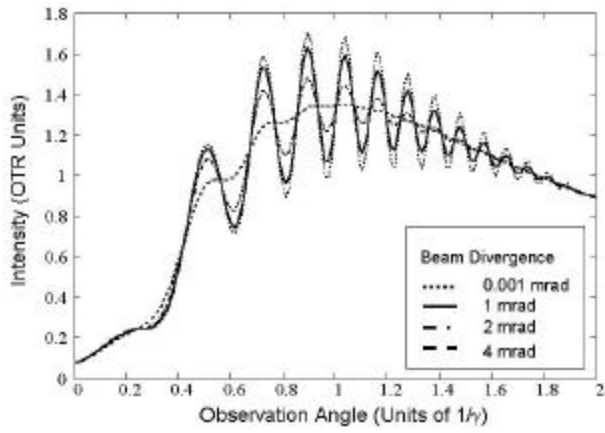


Figure 4: The effect of divergence on the total intensity of ODR-OTR for a two foil interferometer, whose foils are separated by $d = 1.5$ mm. The presence of fringes indicates a coherent addition of intensities from the first and second foils.

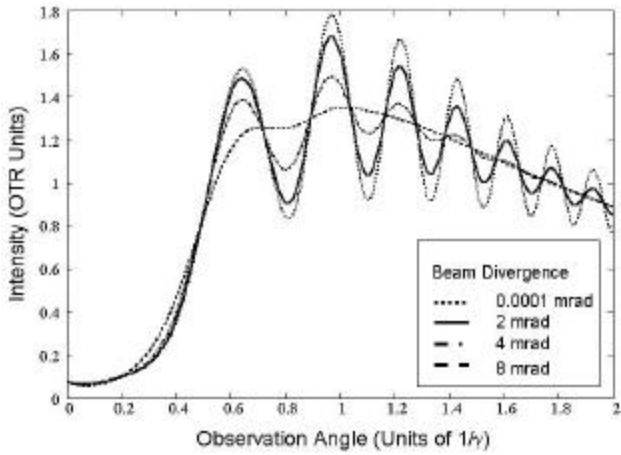


Figure 5: Similar to Figure 4 except the interfoil spacing d is reduced to 0.75 mm. The result is an increased sensitivity to higher values of divergence (2- 8 mrad).

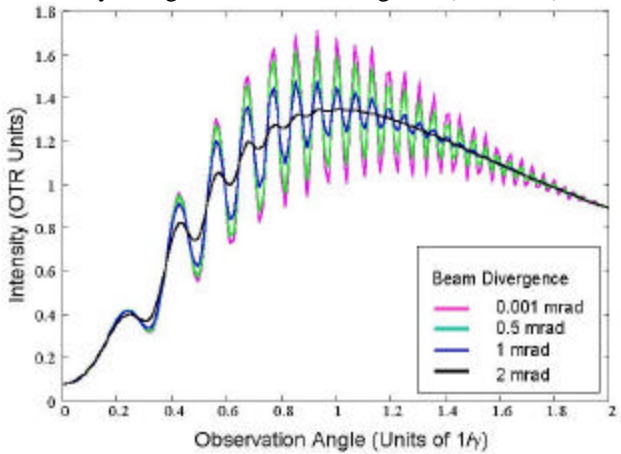


Figure 6: Similar to Figures 4 and 5 except now d is increased to 3 mm. This results in an increased sensitivity to lower values of divergence (0.5 – 2.0 mrad).

4 EXPERIMENTAL CONSIDERATIONS

If the OTR radiation is projected on a two dimensional detector (e.g. a CCD camera), the single foil OTR intensity distribution on the detector can be written as:

$$dW(\mathbf{j}, \mathbf{r}, \mathbf{w}) = \frac{e^2 r^3 dr d\mathbf{j} d\mathbf{w}}{p^2 c (r_0^2 + r^2)^2},$$

where the radius r_0 corresponds to the angle γ_0^{-1} . For good resolution of the fringes, the detector should have about 100 resolution points (pixels) in an angular interval $2\gamma^{-1}$.

The maximum energy per pixel, per electron in the wavelength interval $\Delta\lambda$ is $Q = 1.6 \times 10^5 e^2 \lambda^{-2} \Delta\lambda$. Considering the angular range $0 < \theta < 2/\gamma$, and for $\lambda = 750$ nm, $\Delta\lambda = 40$ nm, the total power in Watts is $P_{Tot} = 1.9 \times 10^4 J$, where J is the average beam current, and the average power per pixel, $P_{Avg} = 1.5 \times 10^9 J$. The typical average current of the MRFEL 8 MeV accelerator at University of Maryland is $J_{avg} = 6 \mu A$. This current can produce an average OTR-ODR power per pixel, $P_{pixel} \sim 10^{-15}$ watts, which is well within the range of detection for a sensitive CCD camera. ODR-OTR interferences should then be easily imaged with a CCD camera and frame integration.

5 CONCLUSIONS

Measurement of the divergence of a low energy low emittance electron beam can be made by measuring the visibility of ODR-OTR interference fringes produced by the unscattered portion of the beam passing through a perforated front foil of an ODR-OTR interferometer. These interference fringes are clearly visible above the incoherent background light from the scattered portion of the beam and can be used to measure the 2 mrad divergence expected for the 8 MeV MRFEL electron beam.

6 REFERENCES

- [1] R. B. Fiorito and D. W. Rule, "Optical Transition Radiation Beam Emittance Diagnostics", in AIP Conference Proceedings No. 319, R. Shafer editor, (1994).
- [2] M. L. Ter-Mikaelian, **High Energy Electromagnetic Processes in Condensed Media**, Wiley-Interscience, New York, NY (1972).
- [3] R. B. Fiorito and D. W. Rule, "Diffraction Radiation Diagnostics for Moderate to High Energy Charged Particle Beams", *Nuc. Instrum. and Meth. B*, 173, 67-82 (2001).
- [4] V. Verzilov, "Transition Radiation in the Pre-wave Zone", *Phys. Lett. A*, 273, 135-140 (2000).